0021-972X/05/$15.00/0
Printed in U.S.A.

The Journal of Clinical Endocrinology & Metabolism 90(12):6508–6515

doi: 10.1210/jc.2005-1258

In Vivo Assessment of Trabecular Bone Microarchitecture by High-Resolution Peripheral Quantitative Computed Tomography

Stephanie Boutroy, Mary L. Bouxsein, Francoise Munoz, and Pierre D. Delmas

INSERM Research Unit 403 (S.B., F.M., P.D.D.), and Claude Bernard University of Lyon, 69437 Lyon, France; and Orthopedic Biomechanics Laboratory (M.L.B.), Beth Israel Deaconess Medical Center, Boston, Massachusetts 02215

Context: Assessment of trabecular microarchitecture may enhance the prediction of fracture risk and improve monitoring of treatment response. A new high-resolution peripheral quantitative computed tomography (HR-pQCT) system permits *in vivo* assessment of trabecular architecture and volumetric bone mineral density (BMD) at the distal radius and tibia with a voxel size of 82 μm^3.

Objective and Patients: We determined the short-term reproducibility of this device by measuring 15 healthy volunteers three times each. We compared HR-pQCT measurements in 108 healthy premenopausal, 113 postmenopausal osteopenic, and 35 postmenopausal osteoporotic women. Furthermore, we compared values in postmenopausal osteopenic women with (n = 35) and without previous fracture history (n = 78).

Design and Setting: We conducted a cross-sectional study in a private clinical research center.

Intervention and Main Outcome Measure: We took HR-pQCT measurements of the radius and tibia. Femoral neck and spine BMD were measured in postmenopausal women by dual-energy x-ray absorptiometry.

Results: Precision of HR-pQCT measurements was 0.7–1.5% for total, trabecular, and cortical densities and 2.5–4.4% for trabecular architecture. Postmenopausal women had lower density, trabecular number, and cortical thickness than premenopausal women ($P < 0.001$) at both radius and tibia. Osteoporotic women had lower density, cortical thickness, and increased trabecular separation than osteopenic women ($P < 0.01$) at both sites. Furthermore, although spine and hip BMD were similar, fractured osteopenic women had lower trabecular density and more heterogeneous trabecular distribution ($P < 0.02$) at the radius compared with unfractured osteopenic women.

Conclusion: HR-pQCT appears promising to assess bone density and microarchitecture at peripheral sites in terms of reproducibility and ability to detect age- and disease-related changes. (***J Clin Endocrinol Metab* 90: 6508–6515, 2005**)

MEASUREMENT OF AREAL bone mineral density (BMD) by dual-energy x-ray absorptiometry (DXA) is presently the accepted method for diagnosis of osteoporosis and prediction of fracture risk. However, recent clinical observations have highlighted some limitations of areal BMD measurements. For instance, half of incident fractures occur in women with BMD values above the World Health Organization (WHO)-defined diagnostic threshold for osteoporosis (1–3). Furthermore, changes in BMD after osteoporosis therapy explain only a small proportion of the reduction in vertebral fracture risk (4, 5). Because osteoporosis is characterized both by low bone mass and microarchitectural deterioration, it has been suggested that *in vivo* assessment of trabecular bone microarchitecture may improve the prediction of fracture risk and the ability to monitor the response to therapeutic intervention (6).

In vivo three-dimensional quantification of trabecular structure by either high-resolution peripheral quantitative computed tomography (HR-pQCT) or micro-magnetic resonance imaging (μMRI) was first introduced over 10 yr ago (7–9). In these initial imaging systems, the nominal isotropic resolution was 170 μm for HR-pQCT, and 80–200 μm in plane with a slice thickness of 400–700 μm for μMRI. Since then, technical advances have improved the spatial resolution of μMRI markedly, with recent studies achieving nominal resolutions of 137 × 137 μm in plane with a slice thickness of 350 μm (10). Additional advances have led to the introduction of a new HR-pQCT system that permits *in vivo* assessment of trabecular architecture and volumetric BMD at the distal radius and tibia with a nominal isotropic voxel size of 82 μm (11).

The overall aim of our study was to evaluate the clinical performance of this new HR-pQCT system. Specifically, we determined the short-term reproducibility of density and architecture measurements, assessed the correlation among the parameters, and compared density and architectural parameters from healthy premenopausal, osteopenic postmenopausal, and osteoporotic postmenopausal women. We also compared parameters in osteopenic postmenopausal women with and without a history of fracture.

First Published Online September 27, 2005

Abbreviations: BMD, Bone mineral density; BV, bone volume; CSA, cross-sectional area; μCT, microcomputed tomography; CTh, cortical thickness; CV, coefficient(s) of variation; D, volumetric bone density; DXA, dual-energy x-ray absorptiometry; HA, hydroxyapatite; HR-pQCT, high-resolution peripheral quantitative computed tomography; μMRI, micro-magnetic resonance imaging; RMS, root mean square; TbN*, trabecular number; TbSp, trabecular separation; TBSp SD, intra-individual distribution of separation; TbTh, trabecular thickness; TV, trabecular volume.

JCEM is published monthly by The Endocrine Society (http://www.endo-society.org), the foremost professional society serving the endocrine community.

Subjects and Methods

Subjects

To assess short-term reproducibility, 15 healthy women (aged 21–47 yr) underwent three separate HR-pQCT scans of the distal radius and tibia within a 1-month period (12).

To determine differences in bone density and microarchitecture between healthy individuals and those with osteoporosis, we evaluated three groups of women: premenopausal, postmenopausal osteopenic, and postmenopausal osteoporotic. The premenopausal group comprised 108 healthy individuals (aged 19–45 yr) who had no conditions known to affect bone or mineral metabolism. The postmenopausal group comprised 148 individuals who had not been menstruating for at least 1 yr. Patients were excluded if they had known current metabolic disorders other than osteoporosis. Based on the lower of their BMD measurements at the lumbar spine or proximal femur, these women were classified as osteopenic ($-1 <$ T-score < -2.5; n = 113 women, aged 52–88 yr) or osteoporotic (T-score ≤ -2.5; n = 35 women, aged 61–82 yr). Measurements at the wrist and at distal tibia were excluded in nine and six women, respectively, because of patient motion. This resulted in a final sample of 106 osteopenic women with HR-pQCT measurements at the distal radius, 109 osteopenic women with HR-pQCT scans at the distal tibia, and 33 osteoporotic women with HR-pQCT scans at the distal radius and at the distal tibia. All measurements from the premenopausal group were included in the final analyses. Measurements were usually performed at the nondominant limb unless there was a history of fracture on that limb, in which case the nonfractured limb was measured.

Personal history of fractures was recorded by a questionnaire. Because of the low number of subjects having had fractures in the premenopausal and postmenopausal osteoporotic groups, differences between individuals with and without a personal history of fracture after the age of 45 yr, excluding those of the face, skull, fingers, and toes, were analyzed in the postmenopausal osteopenic group only. Thus, among the 106 and 109 osteopenic women with valid HR-pQCT scans at the distal radius and distal tibia, respectively, 35 reported at least one previous fracture (44 fractures in total). Fracture types included wrist and distal forearm (n = 18), forearm (n = 5), humerus (n = 4), metacarpal (n = 1), femur (n = 1), patella (n = 1), lower leg (n = 5), ankle (n = 4), metatarsal (n = 3), and ribs (n = 2).

The protocol was approved by an independent Ethics Committee, and all patients gave written informed consent before participation.

Measurement of BMD and bone microarchitecture

BMD (g/cm^2) at the lumbar spine and femoral neck was measured in postmenopausal women using DXA (Hologic QDR4500; Hologic, Bedford, MA).

Volumetric BMD and microarchitecture were measured at the distal radius and distal tibia using a three-dimensional HR-pQCT system (XtremeCT; Scanco Medical AG, Bassersdorf, Switzerland). This system uses a two-dimensional detector array in combination with a 0.08-mm point-focus x-ray tube, enabling the simultaneous acquisition of a stack of parallel CT slices with a nominal resolution (voxel size) of 82 μm. The following settings were used: effective energy of 60 kVp, x-ray tube current of 95 mA, and matrix size of 1536×1536.

At each skeletal site, 110 CT slices were obtained, thus delivering a three-dimensional representation of approximately 9 mm in the axial direction. The arm or leg of the patient was immobilized during the examination in an anatomically formed carbon fiber shell. An anteroposterior scout view was used to define the measurement region. Briefly, a reference line was manually placed at the endplate of the radius and tibia, as shown in Fig. 1A. The first CT slice was 9.5 mm and 22.5 mm proximal to the reference line for the distal radius and distal tibia, respectively. The effective dose was less than 3 μSv per measurement (11) with a measurement time of 2.8 min. Attenuation data were converted to equivalent hydroxyapatite (HA) densities. Quality control, based on Shewart rules, was monitored by daily scans of a phantom containing rods of HA (densities of 0, 100, 200, 400, and 800 mg HA/cm^3) embedded in a soft-tissue equivalent resin (QRM, Moehrendorf, Germany).

Methods used to process the CT data have been previously described in detail by Laib and colleagues (13). Briefly, the entire volume of interest was automatically separated into a cortical and trabecular region using a threshold-based algorithm. The threshold used to discriminate cortical from trabecular bone was set to one third of the apparent cortical bone density value (D_{cort}). Mean cortical thickness (CTh) was defined as the mean cortical volume divided by the outer bone surface. Trabecular bone density (D_{trab}) in mg HA/cm^3 was computed as the average mineral density within the trabecular volume of interest. Trabecular bone volume (BV) fraction [BV/trabecular volume (TV), %] was then derived from trabecular density assuming fully mineralized bone to have a mineral density of 1.2 g HA/cm^3 [*i.e.* BV/TV (%) = $100 \times (D_{trab}$ (mg $HA/cm^3)/1200$ mg $HA/cm^3)$]. Because the thickness of individual trabeculae cannot be measured accurately because of partial volume effects, a thickness-independent algorithm was used to assess trabecular structure (14, 15). First, a mid-axis transformation method was used to identify trabecular elements and the distance between them assessed three-dimensionally using the distance transform method (16). Trabecular number (TbN*, mm^{-1}) was defined as the inverse of the mean spacing of the mid-axes and is thus truly three-dimensional and does not depend on *a priori* assumptions regarding the plate- or rod-like nature of the underlying structure. Trabecular thickness (TbTh, μm) and separation (TbSp, μm) were derived from BV/TV and TbN* using standard methods from histomorphometry (*i.e.* TbTh = (BV/TV) /TbN* and TbSp = $(1 - BV/TV)/TbN^*$) (17). Distance transformation techniques also enable the calculation of intra-individual distribution of separation (TbSp SD, μm), quantified by the SD of the separation, a parameter reflecting the heterogeneity of the trabecular network (18). The values for trabecular architecture parameters are highly correlated with values obtained with a 20-μm resolution QCT device *in vitro*, although trabecular thickness is significantly lower with the HR-pQCT than with the 20-μm-resolution QCT (personal communication from Scanco Medical AG).

For follow-up measurements, an algorithm automatically uses the cross-sectional area (CSA, mm^2) within the periosteal boundary of the radius or tibia to match the volumes of interest on the baseline and follow-up scans, and thus only the bone volume common to the previous scan(s) is used to assess density and microarchitectural measurements (19). Hence, of the initial 110 slices, on average 103 (range, 91–108) were analyzed in the follow-up scans.

The outcome variables used in our analyses included volumetric bone density (g HA/cm^3) for entire (D_{tot}), trabecular (D_{trab}), and cortical (D_{cort}) regions; cortical thickness (CTh, μm); and trabecular bone volume fraction (BV/TV, %), thickness (TbTh, μm), number (TbN*, mm^{-1}), separation (TbSp, μm), and intra-individual distribution of separation (TbSp SD, μm).

Statistical analysis

For each subject in the reproducibility study, a coefficient of variation (CV) calculated as the SD of the three repeated measurements divided by the subject mean. Furthermore, the short-term precision errors were then calculated as root-mean-square (RMS) average of the precision errors for each of the subjects. The relationships between density and architecture were studied using Pearson or Spearman correlation, depending on the distribution of variables. The differences among premenopausal, postmenopausal osteopenic, and postmenopausal osteoporotic individuals were assessed by ANOVA or by a Kruskal-Wallis test (two-tailed tests), followed, when significant, by Student's *t* test or Wilcoxon signed rank test for pair-wise comparisons (one-side tests). Finally, differences between the postmenopausal osteopenic women with and without fracture history were assessed by Student's *t* test or Wilcoxon signed rank test (one-side tests). For the correlation between HR-pQCT parameters, the Bonferroni correction led us to consider statistical significance at $P < 0.02$. All statistical analyses were performed on SPSS software (version 12.0).

Results

Precision of HR-pQCT

Reproducibility (RMS-CV) of density (total, trabecular, and cortical) measurements ranged from 0.7–1.5% (Table 1). In comparison, the reproducibility of structural parameters (trabecular number, thickness, separation, and distribution and cortical thickness) was slightly lower, with RMS-CVs ranging from 0.9–4.4% (Table 1). Measurement reproducibility was similar at the distal radius and distal tibia.

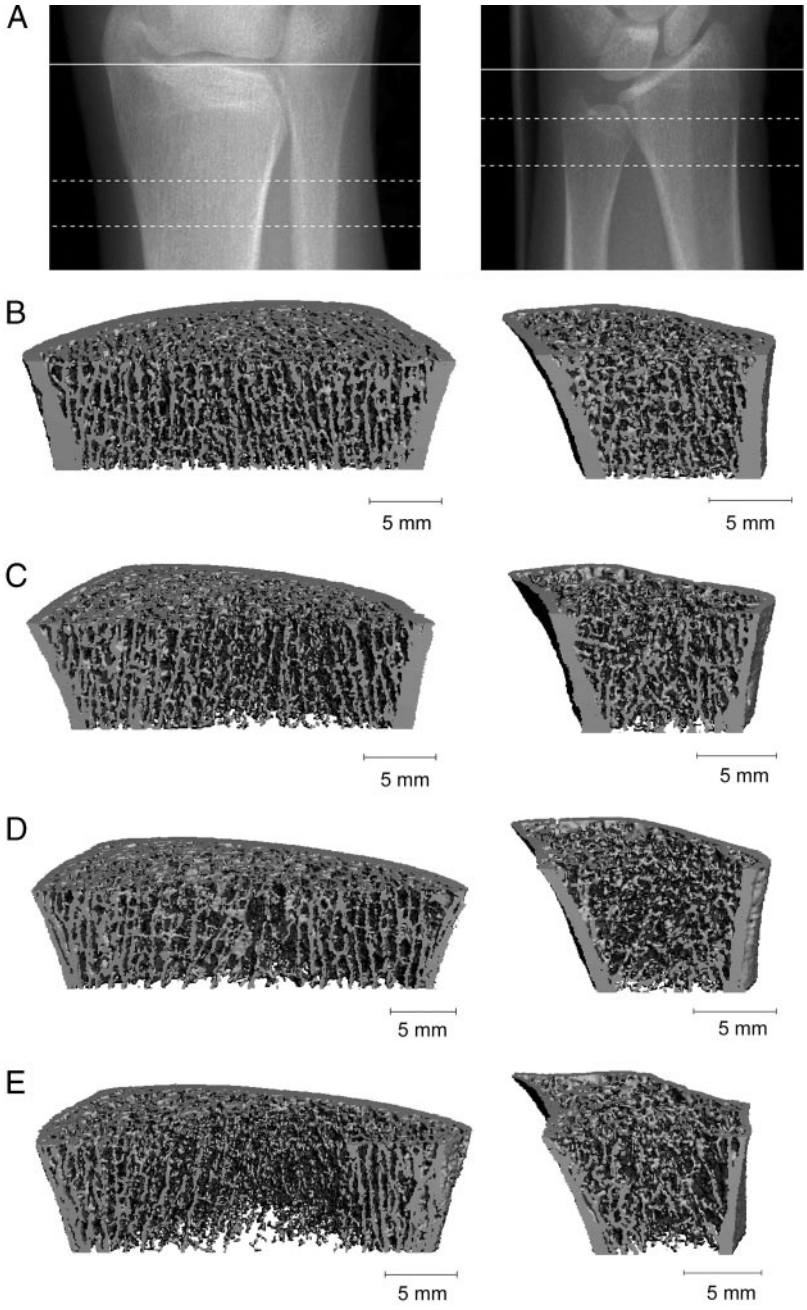

FIG. 1. Representative images of the tibia (*left*) and radius (*right*). A, Scout view demonstrating the reference line position (*solid line*) and the measurement site (between *dotted lines*); B–E, images from a premenopausal (B), postmenopausal osteopenic (C), postmenopausal osteoporotic (D), and postmenopausal severe osteoporotic (E) subject.

Association between age, density, and microarchitecture

The relationships among age, density, and architecture parameters are shown in Table 2. We observed a significant age-related decline in total, trabecular, and cortical bone density at the distal radius ($r = -0.50$ to -0.67) and distal tibia ($r = -0.46$ to -0.79). Architectural parameters were also significantly correlated with age ($|r| = 0.35–0.65$ and $|r| = 0.28–0.65$, respectively, at the radius and tibia). When the analysis was restricted to the population-based sample of 108 premenopausal women, aged 19–45 yr, there was no significant correlation with age for any parameters (data not shown). As expected, total density was strongly correlated to both trabecular and cortical density ($r = 0.80–0.83$ for both). In contrast, trabecular and cortical densities were only modestly related to each other. Trabecular density was strongly correlated to trabecular architectural measurements at both the distal radius ($|r| = 0.78–0.91$) and tibia ($|r| = 0.71–0.75$). Cortical density was highly correlated with cortical thickness but weakly correlated with trabecular architecture. Height and weight were moderately correlated with the cross-sectional bone area at both sites but were only poorly or not significantly correlated with the other parameters.

Comparison of premenopausal and postmenopausal osteopenic and osteoporotic women

Mean values and statistical comparisons among premenopausal, postmenopausal osteopenic, and postmenopausal osteoporotic women are shown in Table 3, and representa-

TABLE 1. Reproducibility of density and structural measurements at the distal radius and distal tibia

	Distal radius		Distal tibia	
	Mean ± SD	CV (%)	Mean ± SD	CV (%)
D_{tot} (mg HA/cm^3)	338 ± 57	0.9	320 ± 39	1.3
D_{cort} (mg HA/cm^3)	902 ± 47	0.7	919 ± 33	0.9
D_{trab} (mg HA/cm^3)	160 ± 24	1.0	179 ± 28	1.5
BV/TV (%)	13.4 ± 2.0	1.0	14.9 ± 2.4	1.5
TbN* (mm^{-1})	1.7 ± 0.2	3.0	1.7 ± 0.2	3.8
TbTh (μm)	76 ± 8	3.2	89 ± 11	4.4
TbSp (μm)	500 ± 58	2.8	510 ± 68	4.3
TbSp SD (μm)	193 ± 24	2.5	218 ± 41	3.3
CTh (μm)	824 ± 148	1.2	1182 ± 130	0.9

CV were calculated from three repeated measurements with repositioning on 15 individuals aged 21–47 yr.

tive three-dimensional images in Fig. 1, B–E. The results of ANOVA and Kruskal-Wallis test showed differences between the three groups for all HR-pQCT parameters except for mean cross-sectional area ($P < 0.001$). Postmenopausal osteopenic and osteoporotic women did not differ in age, height, or weight. At both the radius and tibia, all parameters, except for mean cross-sectional area, were significantly different between premenopausal and postmenopausal women. Specifically, trabecular and cortical density were 19–37% and 11–18%, respectively, lower in postmenopausal than premenopausal women ($P < 0.001$ for all). Postmenopausal women also had lower trabecular number (−12 to −23%; $P < 0.001$) and thickness (−8 to −19%; $P < 0.001$), decreased cortical thickness (−28 to −41%; $P < 0.001$), and increased trabecular separation (21–38%; $P < 0.001$) and intra-individual distribution of separation (53–83%, $P < 0.001$) compared with premenopausal women.

Comparing postmenopausal osteopenic and osteoporotic women, nearly all density and architectural parameters were significantly different, with the exception of cortical density ($P = 0.088$). After the Bonferroni correction, differences were borderline significant for the following parameters: trabecular number ($P = 0.027$) and intra-individual distribution of separation ($P = 0.022$) at the radius and trabecular thickness ($P = 0.029$) at the tibia (Table 3). Compared with those classified as osteopenic, osteoporotic women had lower bone density (−5 to −18%), decreased trabecular number (−10% at the tibia) and thickness (−10% at the radius), increased trabecular separation (+9 to +12%) and intra-individual distribution of separation (+19% at the tibia), and decreased cortical thickness (−15 to −18%) ($P < 0.02$ for all).

Discrimination of osteopenic women with and without history of fracture

Osteopenic women with and without a history of fracture did not differ with regard to age, height, weight, years since menopause, BMD of the lumbar spine and femoral neck, and HR-pQCT measurements at the distal tibia (Table 4). In contrast, at the distal radius, total density (−10.0%; $P = 0.015$), cortical density (−3.4%; $P = 0.042$), trabecular density (−12.3%; $P = 0.018$), and trabecular number (−8.5%; $P = 0.037$) were significantly lower and trabecular separation (+12.8%; $P = 0.027$) and intra-individual distribution of separation (+25.6%; $P = 0.011$) were significantly higher in women with a history of fracture compared with those with no previous fracture (Fig. 2). After the Bonferroni correction, differences were borderline or no more significant for the following parameters: cortical density, trabecular number, and trabecular separation.

Discussion

In this study we evaluated the clinical performance of a new HR-pQCT system by determining short-term reproducibility, correlation among the parameters, and differences among premenopausal, postmenopausal osteopenic, and postmenopausal osteoporotic women. We also compared the measurements in osteopenic postmenopausal women with and without a history of fracture.

We found that the short-term reproducibility of HR-pQCT parameters was quite similar at the distal radius and distal tibia, with CVs less than 1.5% for bone density and from 2.5–4.4% for trabecular architecture. It should be noted that our precision data were generated in healthy individuals, and the values may be higher among osteoporotic subjects. Nonetheless, the reproducibility for density measurements by HR-pQCT is similar to that reported for distal and ultra-

TABLE 2. Correlation matrix for age, height, weight, density, and microarchitectural features at the distal radius (*top half* of table) and distal tibia (*bottom half* of table)

	Age	Height	Weight	D_{tot}	D_{trab}	D_{cort}	BV/TV	TbTh	TbN*	TbSp	TbSp SD	CTh	CSA
Age		−0.45	0.18[c]	−0.61	−0.50	−0.67	−0.50	−0.35	−0.50	0.51	0.58	−0.65	0.11[c]
Height	−0.45		0.30	NS	0.13[c]	0.19	0.13[c]	NS	0.16[c]	−0.15[c]	−0.16[c]	0.18[c]	0.47
Weight	0.18[c]	0.30		−0.13[c]	NS	NS	NS	−0.11[c]	NS	NS	NS	NS	0.34
D_{tot}	−0.64	NS	−0.17[c]		0.80	0.83	0.80	0.73	0.61	−0.65	−0.67	0.92	−0.56
D_{trab}	−0.46	0.21	NS	0.82		0.47	>0.99[a]	0.78[b]	0.86	−0.91[b]	−0.87	0.55	−0.28
D_{cort}	−0.79	0.28	−0.20	0.80	0.43		0.47	0.49	0.34	−0.41	−0.47	0.95	−0.44
BV/TV	−0.46	0.21	NS	0.82	>0.99[a]	0.43		0.78[b]	0.86	−0.91[b]	−0.87	0.55	−0.28
TbTh	−0.28	NS	−0.19[c]	0.65	0.71[b]	0.33	0.71[b]		0.42[b]	−0.50	−0.48	0.55	−0.34
TbN*	−0.36	0.32	0.12[c]	0.45	0.72	0.28	0.72	NS[b]		−0.99[b]	−0.95	0.39	NS
TbSp	0.38	−0.30	NS	−0.53	−0.75[b]	−0.31	−0.75[b]	−0.14[c]	−0.99[b]		0.95	−0.43	0.12[c]
TbSp SD	0.46	−0.33	NS	−0.56	−0.71	−0.41	−0.71	−0.14[c]	−0.93	0.93		−0.48	0.16[c]
CTh	−0.65	0.13[c]	−0.14[c]	0.90	0.54	0.87	0.54	0.46	0.24	−0.30	−0.36		−0.43
CSA	0.14[c]	0.53	0.48	−0.53	−0.26	−0.34	−0.26	−0.45	NS	NS	NS	−0.45	

NS, Not significant.
[a] BV/TV is derived from D_{trab}.
[b] TbTh and TbSp are derived from TbN* and BV/TV (thus from D_{trab}).
[c] $P < 0.05$; all other correlations are significant at $P < 0.001$.

TABLE 3. Mean values for young normal, osteopenic, and osteoporotic women (mean ± SD)

	Premenopausal (n = 108)	Osteopenic (n = 113)	Premenopausal *vs.* osteopenic (%)	Osteoporotic (n = 35)	Premenopausal *vs.* osteoporotic (%)	Osteoporotic *vs.* osteopenic (%)
Age (yr)	34 ± 7	69 ± 7		69 ± 5		NS
Height (m)	165 ± 6	158 ± 6	−4.2[a]	158 ± 8	−4.2[a]	NS
Weight (kg)	60 ± 10	64 ± 10	6.7[a]	62 ± 10	NS	NS
Years since menopause		18.5 ± 7.7		17.6 ± 6.6		NS
Lumbar spine BMD (g/cm^2)		0.89 ± 0.07		0.75 ± 0.04		−16.2[b]
Spine T-score		−1.4 ± 0.6		−2.7 ± 0.4		
Femoral neck BMD (g/cm^2)		0.66 ± 0.06		0.62 ± 0.073		−7.1[b]
Femoral neck T-score		−1.6 ± 0.5		−2.0 ± 0.6		
Distal radius						
D_{tot} (mg HA/cm^3)	330 ± 57	254 ± 62	−23.1[a]	216 ± 40	−34.5[a]	−14.9[b]
D_{cort} (mg HA/cm^3)	904 ± 44	804 ± 81	−11.1[a]	777 ± 72	−14.1[a]	NS
D_{trab} (mg HA/cm^3)	160 ± 33	123 ± 36	−23.1[a]	101 ± 27	−36.7[a]	−17.7[b]
BV/TV (%)	13.4 ± 2.8	10.3 ± 3.0	−23.1[a]	8.5 ± 2.2	−36.7[a]	−17.7[c]
TbN* (mm^{-1})	1.71 ± 0.22	1.44 ± 0.29	−15.5[a]	1.32 ± 0.21	−22.7[a]	−8.5[d,e]
TbTh (μm)	78 ± 11	71 ± 11	−9.3[a]	63 ± 11	−18.5[a]	−10.2[b]
TbSp (μm)	517 ± 88	656 ± 187	26.8[a]	714 ± 140	38.0[a]	8.8[c]
TbSp SD (μm)	212 ± 58	342 ± 201	61.5[a]	340 ± 89	60.3[a]	0.7[d,e]
CTh (μm)	804 ± 149	571 ± 173	−29.0[a]	487 ± 138	−39.4[a]	−14.7[d]
CSA (mm^2)	259 ± 44	264 ± 50	NS	270 ± 37	NS	NS
Distal tibia						
D_{tot} (mg HA/cm^3)	318 ± 50	240 ± 46	−24.5[a]	202 ± 43	−36.3[a]	−15.7[b]
D_{cort} (mg HA/cm^3)	928 ± 32	806 ± 56	−13.1[a]	765 ± 71	−17.5[a]	−5.1[c]
D_{trab} (mg HA/cm^3)	169 ± 34	137 ± 31	−19.3[a]	116 ± 30	−31.3[a]	−14.8[b]
BV/TV (%)	14.1 ± 2.8	11.4 ± 2.6	−19.4[a]	9.7 ± 2.5	−31.2[a]	−14.7[b]
TbN* (mm^{-1})	1.60 ± 0.24	1.42 ± 0.27	−11.6[a]	1.27 ± 0.25	−20.4[a]	−10.0[c]
TbTh (μm)	89 ± 15	82 ± 18	−8.1[a]	77 ± 14	−13.5[a]	−6.1[d,e]
TbSp (μm)	551 ± 97	668 ± 278	21.3[a]	750 ± 227	36.2[a]	12.3[c]
TbSp SD (μm)	240 ± 52	367 ± 359	53.2[a]	438 ± 293	82.7[a]	19.2[b]
CTh (μm)	1232 ± 191	882 ± 220	−28.4[a]	722 ± 240	−41.4[a]	−18.1[b]
CSA (mm^2)	643 ± 104	654 ± 111	NS	692 ± 107	NS	NS

NS, Not significant.
[a] Significantly different from premenopausal, $P < 0.001$, except for weight $P = 0.004$.
[b–d] Significantly different from osteopenic: [b] $P < 0.001$; [c] $P < 0.01$; [d] $P < 0.05$.
[e] Not significant after the Bonferroni correction.

distal radius BMD by DXA (20, 21). The reproducibility of trabecular architecture measurements is also similar to or better than previous studies using a lower-resolution *in vivo* HR-pQCT system (19, 22) or high-resolution MRI (23, 24). Reproducibility of trabecular structure measurement by MRI has been reported to be 2–9%, depending on the specific parameter and analysis algorithm (23, 25, 26). Patient movement and difficulty in matching the analysis volume in repeat studies have been cited as primary error sources for follow-up measurements (23). Patient movement was also a concern in our study, because nine women (3.5%) at the distal radius and six women (2.3%) at the distal tibia were eliminated because of obvious movement artifacts that rendered the scan unsuitable for analysis. Given that several studies have shown that MRI is capable of detecting changes in trabecular structure caused by disease or treatment (24, 26–30), our findings of comparable or better reproducibility in HR-pQCT measurements are encouraging in this regard.

We observed significant age-related changes in density, trabecular structure, and cortical thickness, as evidenced both by correlations with age (Table 2) and by comparing pre- with postmenopausal women (Table 3). At both the distal radius and distal tibia, the correlations between density and age were similar to those recently reported in a large population-based study with a broader age range than our subjects (31). We confirm a number of previous *in vitro* and *in vivo* studies that have reported the decline in trabecular bone density (*i.e.* BV/TV) to be accompanied by declines in trabecular number and thickness (32–34). In our study, the decline in trabecular number was slightly more pronounced than the decline in thickness. Possible explanations for this observation include the possibility that thinner trabeculae are resorbed first, thereby increasing the mean thickness of those remaining and/or by the possibility that the trabeculae that remain adapt to the increased mechanical demand by increasing their size. Similar findings have been noted at the calcaneus, where the rate of age-related declines in trabecular number was reported to be approximately twice that of the decline in trabecular thickness (27). We also observed the expected age-related declines in cortical thickness. Thus, the HR-pQCT measurements appear useful for gaining insight into structural mechanisms underlying various causes of and treatments for skeletal fragility, because they are capable of assessing architecture and density changes in both the cortical and trabecular bone compartments. For example, this may be particularly useful in delineating the subtle compartment-specific effects of mild hyperparathyroidism or intermittent PTH administration (35). Moreover, by assessing individual bone compartments with excellent precision, HR-pQCT may improve the ability to monitor the response to antiresorptive therapy, a critical clinical issue (4).

An interesting finding of our study was the ability of

TABLE 4. Comparison of mean values between postmenopausal osteopenic women with and without history of fracture (mean ± SD)

	Distal radius			Distal tibia		
	Women without fracture (n = 78)	Women with fracture (n = 35)	*P* value	Women without fracture (n = 78)	Women with fracture (n = 35)	*P* value
Age (yr)	68 ± 7	70 ± 5	NS	68 ± 7	70 ± 5	NS
Height (m)	158 ± 6	158 ± 5	NS	158 ± 6	158 ± 5	NS
Weight (kg)	64 ± 10	65 ± 10	NS	64 ± 10	65 ± 10	NS
Years since menopause	18 ± 8	19 ± 7	NS	18 ± 8	19 ± 7	NS
Lumbar spine BMD (g/cm^2)	0.89 ± 0.07	0.89 ± 0.07	NS	0.89 ± 0.07	0.89 ± 0.07	NS
Spine T-score	−1.5 ± 0.7	−1.4 ± 0.6	NS	−1.5 ± 0.7	−1.4 ± 0.6	NS
Femoral neck BMD (g/cm^2)	0.66 ± 0.05	0.66 ± 0.07	NS	0.66 ± 0.05	0.66 ± 0.07	NS
Femoral neck T-score	−1.6 ± 0.4	−1.6 ± 0.6	NS	−1.6 ± 0.4	−1.6 ± 0.6	NS
D_{tot} (mg HA/cm^3)	262 ± 61	236 ± 61	0.015	243 ± 45	232 ± 47	NS
D_{cort} (mg HA/cm^3)	813 ± 80	785 ± 81	0.042[a]	811 ± 57	794 ± 53	NS
D_{trab} (mg HA/cm^3)	128 ± 34	113 ± 36	0.018	138 ± 30	134 ± 32	NS
BV/TV (%)	10.7 ± 2.9	9.4 ± 3.0	0.017	11.5 ± 2.5	11.2 ± 2.7	NS
TbN* (mm^{-1})	1.48 ± 0.28	1.36 ± 0.31	0.037[a]	1.42 ± 0.25	1.39 ± 0.30	NS
TbTh (μm)	72 ± 10	68 ± 14	NS	82 ± 19	81 ± 13	NS
TbSp (μm)	630 ± 170	711 ± 210	0.027[a]	666 ± 308	673 ± 193	NS
TbSp SD (μm)	316 ± 178	397 ± 237	0.011	369 ± 396	363 ± 258	NS
CTh (μm)	590 ± 169	530 ± 175	NS	898 ± 223	844 ± 212	NS
CSA (mm^2)	264 ± 49	265 ± 51	NS	649 ± 108	668 ± 118	NS

NS, Not significant.
[a] Not significant after the Bonferroni correction.

HR-pQCT measurements of trabecular bone density and intra-individual distribution of separation at the distal radius to discriminate between osteopenic women with and without a history of fracture, whereas spine and hip BMD measurements did not (Table 4). Admittedly, these findings must be interpreted with caution because our study had a relatively small sample size with various types of fractures, and thus, our results need to be confirmed in a larger prospective study. Whereas several previous studies have shown that *in vivo* measurements of trabecular structure can be used to identify osteoporotic women with and without fractures and that trabecular structure may improve predictions of fracture risk based on BMD alone, generally the fracture cases in these studies also have lower BMD than controls (34, 36–38). An exception to this is the study by Link *et al*. (39) who demonstrated that MRI-based measurements of trabecular structure differed among cardiac transplant patients with and without vertebral fractures, whereas BMD did not. Moreover, Laib *et al*. (18) have reported that the distribution of trabecular separation (TbSp SD) was the MRI index that was most sensitive for discrimination of individuals with and without spine fractures. Placed in the context of current clinical dilemmas, our preliminary results are intriguing, because over half of osteoporotic fractures occur in women with osteopenia by WHO criteria, and identification of factors that predispose these osteopenic women to fracture is needed (1, 3).

Regarding the personal history of fracture, there were 2-fold more fractures at the arm than at the leg, which may explain why only measurements at the distal radius were able to discriminate among fractured *vs.* unfractured subjects. Moreover, as the radius is not weight bearing, one may

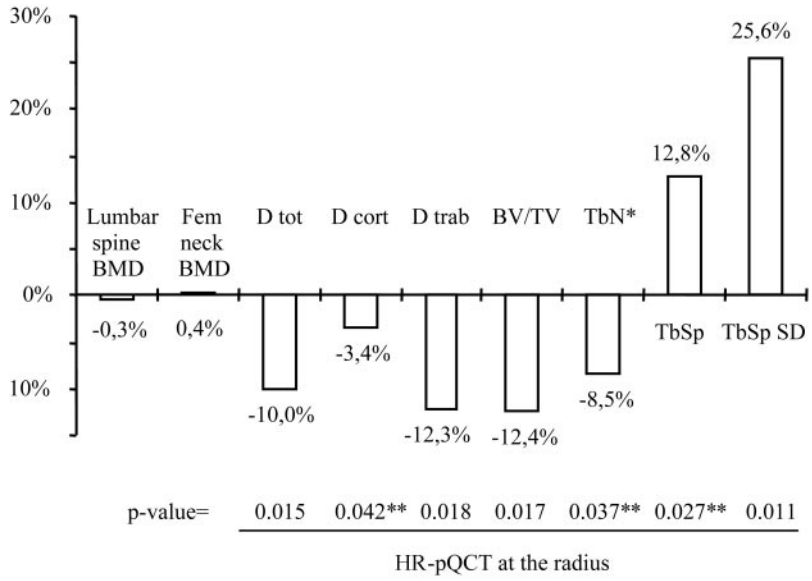

FIG. 2. Percent difference between BMD and HR-pQCT parameters and *P* value between osteopenic women with previous history of fracture compared with those who were fracture free. **, Not significant after the Bonferroni correction.

speculate that there are fewer mechanical stimuli to maintain structural integrity in the face of estrogen deficiency, and perhaps trabecular architectural changes are more rapid and/or more dramatic at the radius than the distal tibia. Additional studies are needed to better understand the utility of each of these skeletal sites with regard to fracture risk prediction.

It should be noted that our study design had several limitations. First, the study was cross-sectional, and therefore the ability of the HR-pQCT measurements to predict fracture risk prospectively and to monitor age-, disease-, and treatment-related changes in bone density or architecture requires additional validation. Second, as mentioned previously, the sample size was relatively small; the premenopausal group comprised 108 individuals, thereby precluding establishment of normal reference values. Moreover, we did not have the ideal population-based sample with equal representation across the lifespan to accurately assess age-related patterns.

There are several technical limitations that should be considered as well. We noted, as have others, moderate to strong correlations between trabecular density and trabecular architecture. These observations must be viewed carefully because in the current study, trabecular density and trabecular number are independently measured, whereas BV/TV, trabecular thickness, and trabecular separation are derived. Additional studies are required to discern the combination of density and architectural features that will be most useful clinically. Moreover, we found that cortical thickness and cortical density were very strongly correlated (Table 2). This high correlation suggests that partial volume effects limit the reliability of cortical density measurements. In support of this view, we note that cortical thickness and density were more strongly correlated at the distal radius ($r^2 = 0.90$), where average cortical thickness ranged from 190-1170 μm, than they were at the distal tibia ($r^2 = 0.76$), where average cortical thickness is higher (280–1790 μm). Removal of cortical surface voxels before computation of cortical density may improve the reliability of the cortical density measurements, which at present should be viewed with caution. Even if the reliability is improved, cortical density measurements will still reflect the combined influence of porosity and the degree of matrix mineralization, because a resolution on the order of 10 μm is required to directly assess cortical porosity in humans (40).

Despite these limitations, the current study has provided new information regarding the potential clinical utility of HR-pQCT measurements with 82-μm isotropic voxel size. Additional studies are required to confirm and extend these preliminary results. Altogether, however, our findings indicate that HR-pQCT appears promising as a technique to assess bone density and trabecular microarchitecture at peripheral skeletal sites, both in terms of reproducibility and ability to detect age- and disease-related changes.

Acknowledgments

We thank Dr. Elisabeth Sornay-Rendu for the recruitment of some of the patients and Betty Vey Marty for valuable technical assistance. We also thank Bruno Koller and Andres Laib of Scanco Medical AG, for their scientific support and for helpful discussions.

Received June 3, 2005. Accepted September 15, 2005.

Address all correspondence and requests for reprints to: Prof. Pierre D. Delmas, INSERM Unit 403, Hôpital Edouard Herriot, Pavillon F, 69437 Lyon Cedex 03, France. E-mail: delmas@lyon.inserm.fr.

This work was supported in part by an unrestricted grant from Eli Lilly to INSERM.

References

1. **Siris ES, Miller PD, Barrett-Connor E, Faulkner KG, Wehren LE, Abbott TA, Berger ML, Santora AC, Sherwood LM** 2001 Identification and fracture outcomes of undiagnosed low bone mineral density in postmenopausal women: results from the National Osteoporosis Risk Assessment. JAMA 286:2815–2822
2. **Stone KL, Seeley DG, Lui LY, Cauley JA, Ensrud K, Browner WS, Nevitt MC, Cummings SR** 2003 BMD at multiple sites and risk of fracture of multiple types: long-term results from the Study of Osteoporotic Fractures. J Bone Miner Res 18:1947–1954
3. **Schuit SC, van der Klift M, Weel AE, de Laet CE, Burger H, Seeman E, Hofman A, Uitterlinden AG, van Leeuwen JP, Pols HA** 2004 Fracture incidence and association with bone mineral density in elderly men and women: the Rotterdam Study. Bone 34:195–202
4. **Delmas PD, Seeman E** 2004 Changes in bone mineral density explain little of the reduction in vertebral or nonvertebral fracture risk with anti-resorptive therapy. Bone 34:599–604
5. **Delmas PD** 2000 How does antiresorptive therapy decrease the risk of fracture in women with osteoporosis? Bone 27:1–3
6. **Ulrich D, van Rietbergen B, Laib A, Ruegsegger P** 1999 The ability of three-dimensional structural indices to reflect mechanical aspects of trabecular bone. Bone 25:55–60
7. **Wehrli FW, Ford JC, Chung HW, Wehrli SL, Williams JL, Grimm MJ, Kugelmass SD, Jara H** 1993 Potential role of nuclear magnetic resonance for the evaluation of trabecular bone quality. Calcif Tissue Int 53(Suppl 1):S162–S169
8. **Muller R, Hildebrand T, Ruegsegger P** 1994 Non-invasive bone biopsy: a new method to analyse and display the three-dimensional structure of trabecular bone. Phys Med Biol 39:145–164
9. **Majumdar S, Genant HK** 1995 A review of the recent advances in magnetic resonance imaging in the assessment of osteoporosis. Osteoporos Int 5:79–92
10. **Wehrli FW, Gomberg BR, Saha PK, Song HK, Hwang SN, Snyder PJ** 2001 Digital topological analysis of in vivo magnetic resonance microimages of trabecular bone reveals structural implications of osteoporosis. J Bone Miner Res 16:1520–1531
11. **Laib A, Hammerle S, Koller B,** A new 100 μm resolution scanner for in vivo 3D-CT of the human forearm and lower leg. 16th International Bone Densitometry Workshop, Annecy, France, 2004
12. **Gluer CC, Blake G, Lu Y, Blunt BA, Jergas M, Genant HK** 1995 Accurate assessment of precision errors: how to measure the reproducibility of bone densitometry techniques. Osteoporos Int 5:262–270
13. **Laib A, Hauselmann HJ, Ruegsegger P** 1998 In vivo high resolution 3D-QCT of the human forearm. Technol Health Care 6:329–337
14. **Laib A, Ruegsegger P** 1999 Comparison of structure extraction methods for in vivo trabecular bone measurements. Comput Med Imaging Graph 23:69–74
15. **Laib A, Ruegsegger P** 1999 Calibration of trabecular bone structure measurements of in vivo three-dimensional peripheral quantitative computed tomography with 28-micron-resolution microcomputed tomography. Bone 24:35–39
16. **Hildebrand T, Ruegsegger P** 1997 Quantification of bone microarchitecture with the structure model index. Comput Methods Biomech Biomed Engin 1:15–23
17. **Parfitt AM, Mathews CH, Villanueva AR, Kleerekoper M, Frame B, Rao DS** 1983 Relationships between surface, volume, and thickness of iliac trabecular bone in aging and in osteoporosis. Implications for the microanatomic and cellular mechanisms of bone loss. J Clin Invest 72:1396–1409
18. **Laib A, Newitt DC, Lu Y, Majumdar S** 2002 New model-independent measures of trabecular bone structure applied to in vivo high-resolution MR images. Osteoporos Int 13:130–136
19. **Laib A, Hildebrand T, Hauselmann HJ, Ruegsegger P** 1997 Ridge number density: a new parameter for in vivo bone structure analysis. Bone 21:541–546
20. **Arlot ME, Sornay-Rendu E, Garnero P, Vey-Marty B, Delmas PD** 1997 Apparent pre- and postmenopausal bone loss evaluated by DXA at different skeletal sites in women: the OFELY cohort. J Bone Miner Res 12:683–690
21. **Rey P, Sornay-Rendu E, Garnero P, Vey-Marty B, Delmas PD** 1994 [Measurement of bone density in the wrist using X-ray absorptiometry: comparison with measurements of other sites]. Rev Rhum Ed Fr 61:619–626 (French)
22. **Muller R, Hildebrand T, Hauselmann HJ, Ruegsegger P** 1996 In vivo reproducibility of three-dimensional structural properties of noninvasive bone biopsies using 3D-pQCT. J Bone Miner Res 11:1745–1750
23. **Gomberg BR, Wehrli FW, Vasilic B, Weening RH, Saha PK, Song HK, Wright AC** 2004 Reproducibility and error sources of micro-MRI-based trabecular bone structural parameters of the distal radius and tibia. Bone 35:266–276
24. **Newitt DC, Majumdar S, van Rietbergen B, von Ingersleben G, Harris ST, Genant HK, Chesnut C, Garnero P, MacDonald B** 2002 In vivo assessment of

architecture and micro-finite element analysis derived indices of mechanical properties of trabecular bone in the radius. Osteoporos Int 13:6–17
25. **Newitt DC, van Rietbergen B, Majumdar S** 2002 Processing and analysis of in vivo high-resolution MR images of trabecular bone for longitudinal studies: reproducibility of structural measures and micro-finite element analysis derived mechanical properties. Osteoporos Int 13:278–287
26. **Pothuaud L, Newitt DC, Lu Y, MacDonald B, Majumdar S** 2004 In vivo application of 3D-line skeleton graph analysis (LSGA) technique with high-resolution magnetic resonance imaging of trabecular bone structure. Osteoporos Int 15:411–419
27. **Ouyang X, Selby K, Lang P, Engelke K, Klifa C, Fan B, Zucconi F, Hottya G, Chen M, Majumdar S, Genant HK** 1997 High resolution magnetic resonance imaging of the calcaneus: age-related changes in trabecular structure and comparison with dual x-ray absorptiometry measurements. Calcif Tissue Int 60:139–147
28. **Link TM, Saborowski, Kisters K, Kempkes M, Kosch M, Newitt D, Lu Y, Waldt S, Majumdar S** 2002 Changes in calcaneal trabecular bone structure assessed with high-resolution MR imaging in patients with kidney transplantation. Osteoporos Int 13:119–129
29. **Benito M, Gomberg B, Wehrli FW, Weening RH, Zemel B, Wright AC, Song HK, Cucchiara A, Snyder PJ** 2003 Deterioration of trabecular architecture in hypogonadal men. J Clin Endocrinol Metab 88:1497–1502
30. **Wehrli FW, Leonard MB, Saha PK, Gomberg BR** 2004 Quantitative high-resolution magnetic resonance imaging reveals structural implications of renal osteodystrophy on trabecular and cortical bone. J Magn Reson Imaging 20: 83–89
31. **Riggs BL, Melton Iii 3rd LJ, Robb RA, Camp JJ, Atkinson EJ, Peterson JM, Rouleau PA, McCollough CH, Bouxsein ML, Khosla S** 2004 Population-based study of age and sex differences in bone volumetric density, size, geometry, and structure at different skeletal sites. J Bone Miner Res 19:1945–1954
32. **Mosekilde L** 1988 Age-related changes in vertebral trabecular bone architecture: assessed by a new method. Bone 9:247–250
33. **Ding M, Hvid I** 2000 Quantification of age-related changes in the structure model type and trabecular thickness of human tibial cancellous bone. Bone 26:291–295
34. **Majumdar S, Genant HK, Grampp S, Newitt DC, Truong VH, Lin JC, Mathur A** 1997 Correlation of trabecular bone structure with age, bone mineral density, and osteoporotic status: in vivo studies in the distal radius using high resolution magnetic resonance imaging. J Bone Miner Res 12:111–118
35. **Zanchetta JR, Bogado CE, Ferretti JL, Wang O, Wilson MG, Sato M, Gaich GA, Dalsky GP, Myers SL** 2003 Effects of teriparatide [recombinant human parathyroid hormone (1–34)] on cortical bone in postmenopausal women with osteoporosis. J Bone Miner Res 18:539–543
36. **Link TM, Majumdar S, Augat P, Lin JC, Newitt D, Lu Y, Lane NE, Genant HK** 1998 In vivo high resolution MRI of the calcaneus: differences in trabecular structure in osteoporosis patients. J Bone Miner Res 13:1175–1182
37. **Wehrli FW, Hwang SN, Ma J, Song HK, Ford JC, Haddad JG** 1998 Cancellous bone volume and structure in the forearm: noninvasive assessment with MR microimaging and image processing. Radiology 206:347–357
38. **Majumdar S, Link TM, Augat P, Lin JC, Newitt D, Lane NE, Genant HK** 1999 Trabecular bone architecture in the distal radius using magnetic resonance imaging in subjects with fractures of the proximal femur. Magnetic Resonance Science Center and Osteoporosis and Arthritis Research Group. Osteoporos Int 10:231–239
39. **Link TM, Lotter A, Beyer F, Christiansen S, Newitt D, Lu Y, Schmid C, Majumdar S** 2000 Changes in calcaneal trabecular bone structure after heart transplantation: an MR imaging study. Radiology 217:855–862
40. **Cooper DM, Matyas JR, Katzenberg MA, Hallgrimsson B** 2004 Comparison of microcomputed tomographic and microradiographic measurements of cortical bone porosity. Calcif Tissue Int 74:437–447

JCEM is published monthly by The Endocrine Society (http://www.endo-society.org), the foremost professional society serving the endocrine community.